Appl. Phys. B 33, 9–16 (1984)

Applied Physics B Photophysics and Laser Chemistry

Transverse Mode Dynamics in a Free-Electron Laser

P. Elleaume[1] and D. A. G. Deacon[2]

LURE, Université de Paris-Sud, F-91405 Orsay, France

[1] CEN Saclay, DPC/SPP/SP, F-91190 Gif, France

[2] Deacon Research, 754 Duncardine Way, Sunnyvale, CA 94087, USA

Received 16 August 1983/Accepted 12 September 1983

Abstract. We derive the most general equations of motion for the electrons and the electromagnetic field in a free-electron laser including the effects of diffraction and pulse propagation. The field evolution is expressed in terms of the amplitudes and phases of a complete set of transverse modes. The analytic solution is given in the small-signal regime, where the theory is shown to be in excellent agreement with a recent experiment at Orsay.

PACS: 42.60, 42.20, 42.55

Stimulated by the original free-electron-laser experiments [1] in 1977, a number of authors have contributed to the development of a purely classical theory for the electron dynamics and the electromagnetic wave growth in these devices. The initial work assumed the light could be represented by a single-frequency plane wave [2, 3]. The first generalization was required to explain the extremely short pulse phenomena observed at Stanford [4, 5]. The inclusion of the longitudinal modes in the theory [6–8] permitted the explanation of the cavity detuning curve, and predicted a range of phenomena in the pulse structure which have yet to be observed. More recently, the theory has been broadened to include the transverse-mode structure of the optical beam [9–15]. Until our work at Orsay [16], no experimental information has been available to test the validity of these so-called 3D theories.

In this paper, we present a new approach to calculating the three-dimensional effects operative in free-electron lasers. The previously mentioned approaches consider the growth of the field $\mathscr{E}(\mathbf{r}, t)$ along the propagation or $\hat{z}$ axis by evaluating its change at each point (x, y), and integrating numerically through the interaction region in the time domain [9–14] or in the frequency domain [15]. These techniques all demand long computer runs if they are to be applied to a real experimental situation. Our approach decomposes the problem into the minimum number of physically observable quantities: the transverse optical modes of the system. The field evolution is expressed in terms of a complete set of orthogonal transverse modes; equations are developed for the propagation of the amplitude and phase of each mode. In physical systems which operate on a few of the lowest-order modes, this approach greatly increases the accuracy, and may reduce the required computer time for the calculation by working in a vector space well matched to the solution of the problem. For the oscillator case, the appropriate choice of modes is the set of eigenmodes of the cavity. For the amplifier, the vector space of modes is determined by the characteristics of the input mode, which is presumably a TEM_{00} Gaussian mode. In either device, an optimum design would result in the excitation of as few of the higher-order modes as possible. The modal decomposition method is therefore well adapted to the prediction and optimization of the operation of the free-electron laser (FEL).

In the first section, we derive, in their most general form, the equations governing the dynamics of the complex mode amplitudes. The subsequent sections reduce these equations to the familiar case of the small signal, low-gain result (Sect. 2). Here, the problem becomes linear, the mode evolution can be described by a matrix transformation, and we retrieve the well known gain equation complete with filling factor. The

theory is then applied to the case of the Orsay experiment, where the results are in excellent agreement with an experiment [16] performed recently which exhibits the off-diagonal terms of the gain matrix.

1. Theoretical Development of the Fundamental Equations

The FEL system is properly described by the coupled Maxwell and Lorentz force equations. From these, we shall derive a self-consistent set of equations describing the electron and the transverse optical mode dynamics. We use the dimensionless notation originally developed by Colson (in fact this work is a generalization of Colson's work to include transverse modes and we shall stay as close as possible to his original notation). Let us recall his main equations describing the field and electron dynamics in the slowly varying phase and amplitude approximation [18]:

$$\frac{dv}{d\tau} = a' \cos(\zeta + \phi), \tag{1}$$

$$\frac{d\zeta}{d\tau} = v, \tag{2}$$

$$\frac{da'}{d\tau} = -r' \langle e^{-i\zeta} \rangle_{\zeta_0, v_0}, \tag{3}$$

where

$$\zeta(t) = (k + k_0) z(t) - \omega t \tag{4}$$

is the dimensionless electron phase,

$$v(t) = L[(k + k_0) \beta_z(t) - k] \tag{5}$$

the dimensionless resonance parameter,

$$\tau = \frac{ct}{L} \tag{6}$$

the dimensionless interaction time,

$$a'(z,t) = \frac{4\pi e N L K E(z,t) e^{i\phi(z,t)}}{\gamma^2 mc^2} \tag{7}$$

the dimensionless complex field amplitude, and

$$r'(z(t)) = \frac{8\pi^2 e^2 N L^2 K^2 \varrho(z(t))}{\gamma^3 mc^2} \tag{8}$$

the dimensionless gain parameter.

Here we consider an N-period helical undulator of length L, magnetic period $\lambda_0 = 2\pi/k_0$, peak magnetic field B, and deflection parameter $K = 93.4\,B$ [Gauss] λ_0 [cm]. An electron beam of energy γmc^2, and number density ϱ travels along the axis of the undulator; an individual electron has longitudinal coordinate $z(t)$ and longitudinal velocity $c\beta_z(t)$ at time t. A helically polarized *plane wave* of wavelength $\lambda = 2\pi/k$, frequency ω, and electric field $\mathscr{E}(z,t) = E(z,t) \exp\{i[kz - \omega t + \phi(z,t)]\}$ interacts with the electrons. In (3), $\langle \rangle_{\zeta_0 v_0}$ is the average over the initial phase ζ_0 and resonance parameter v_0 of the electron population at the position z.

Equations (1, 2) are derived directly from the Lorentz force equation and describe the effect of the radiation field on the electrons. The work done by the longitudinal field on the electrons is neglected here, which is a good approximation provided that the modes are not too divergent [14] $\lambda/\omega_0 \ll 2\pi^2 KN/\gamma$. Equation (3) is derived from the Maxwell equations and describes the effect of the electron on the radiation field. The set (1), (2), and (3) is *self-consistent.* Indeed, those equations are very close to being the most general classical equations describing the FEL dynamics. They apply to high and low gain devices ($r' \gg 1$ or $r' \ll 1$), high field and low field cases ($a' \gg 1$ or $a' \ll 1$), and include the effects of multiple longitudinal modes (laser lethargy effects) through the $\hat{z}$ dependence of r', E, and ϕ. Slight modifications allow their extension to the cases of:

- the planar undulator [19],
- the tapered undulator [18],
- the optical klystron [14], and
- space charge effects [19].

However, the plane-wave approximation cannot accurately describe the transverse effects produced by the finite transverse extent of the optical mode and the electron beam. A filling factor calculated with an ad-hoc overlap integral can be added to the results of this calculation, and gives satisfactory results in the small signal regime only so long as one is not interested in the exact transverse field profile.

To relieve this last restriction on the theory, we assume the field to be described in free space by the paraxial wave equation [20]:

$$\left(\frac{\partial^2}{\partial x^2} + \frac{\partial^2}{\partial y^2} - 2ik\frac{\partial}{\partial z}\right) E(\mathbf{r},t) e^{i\phi(\mathbf{r},t)} = 0. \tag{9}$$

This equation is derived from the wave equation $(\nabla^2 - c^{-2}\partial^2/\partial t^2)\mathscr{E} = 0$ in the slowly varying amplitude and phase approximation, and has been widely used in laser field calculations [17, 20]. The general solution of (9) can be expressed as a linear combination of a complete set of orthogonal modes. If we define these modes by the complex amplitude $E_m \exp(i\psi_m)$, where E_m is real and m is the generalized index of the mode (in the two-dimensional transverse space we consider, m represents two integer numbers), the most general expression for the field is

$$E(\mathbf{r},t) e^{i\phi(\mathbf{r},t)} = \sum_m c_m(t)\, E_m(\mathbf{r}) e^{i\psi_m(\mathbf{r})}, \tag{10}$$

where c_m is complex and time-independent in free

space. The orthogonality relation reads

$$\int \frac{dx\,dy}{\pi w_0^2} E_m e^{i\psi_m} E_n e^{-i\psi_n} = \delta_{mn}, \tag{11}$$

where we have chosen a convenient normalization which makes the E_m dimensionless. The modes can be chosen in a variety of symmetries, but it is useful to exhibit their specific form in cylindrical symmetry:

$$E_{pl}(\mathbf{r}) = \sqrt{\frac{2^{l+2}p!}{(p+l)!\,(1+\delta_{0l})}} \frac{w_0}{w(z)} \left(\frac{r}{w(z)}\right)^l \begin{Bmatrix} \cos l\theta \\ \sin l\theta \end{Bmatrix} \cdot L_p^l\left(\frac{2r^2}{w^2(z)}\right) e^{-r^2/w^2(z)}, \tag{12}$$

$$\psi_{pl}(\mathbf{r}) = \frac{kr^2}{2R(z)} - (2p+l+1)\tan^{-1}\frac{z}{z_0}, \tag{13}$$

where r is the radial and θ is the azimuthal coordinate, w_0 is the beam waist, $L_p^l(2r^2/w^2)$ is the associated Laguerre polynomial, and

$$w^2(z) = w_0^2\left(1 + \frac{z^2}{z_0^2}\right), \tag{14}$$

$$R(z) = z\left(1 + \frac{z_0^2}{z^2}\right), \tag{15}$$

$$z_0 = \frac{\pi w_0^2}{\lambda}. \tag{16}$$

These modes are very useful for the case of a cylindrical electron beam aligned to the axis of the light beam. For an ellipsoidal electron beam profile, or off-axis electron injection, the rectangular eigenmodes are more appropriate. Although we will use the cylindrical modes in the examples, we proceed with the general theoretical development which makes no assumptions on the specific form of the modes.

In FEL, the coefficients in (10) become time dependent. We wish to calculate the evolution of the amplitude and phase of these mode coefficients. Proceeding through the derivation of (1–3), making only the slowly varying amplitude and phase approximation, but now using (10) and (11), we find

$$\frac{\partial \nu}{\partial \tau} = \sum_m |a_m| E_m \cos(\zeta + \psi_m + \phi_m), \tag{17}$$

$$\frac{\partial \zeta}{\partial \tau} = \nu, \tag{18}$$

$$\frac{\partial a_m}{\partial \tau} = -\int \frac{dx\,dy}{\pi w_0^2} r E_m e^{-i\psi_m} \langle e^{-i\zeta} \rangle_{\zeta_0 \nu_0}, \tag{19}$$

where we have made the new definitions

$$a_m(z,t) \equiv \frac{4\pi e N L K}{\gamma^2 mc^2} c_m(z,t), \tag{20}$$

$$r(\mathbf{r},t) \equiv \frac{8\pi^2 e^2 N L^2 K^2}{\gamma^3 mc^2} \varrho(\mathbf{r},t), \tag{21}$$

$$c_m(z,t) = |c_m(z,t)|\, e^{i\phi_m(z,t)}. \tag{22}$$

As before, (17) and (18) describe the effect of the radiation field on the electrons, and (19) describes the growth or decay of the radiation field due to its interaction with the electrons. The change in (17) is quite straightforward. Equation (19) shows clearly the fact that the growth in the m^{th} mode amplitude and phase is given by the operlap integral of the inphase and out-of-phase components of the charge density with the complex conjugate of that mode, as one would expect. We note that the only assumptions made on the modes $E_m \exp(i\psi_m)$ used in (17–19) are orthogonality and completeness. This means these equations are also valid for the cases of waveguide modes and dielectrically loaded cavities. In this case, w_0 is no longer the mode waist in the usual Gaussian sense, but is defined by (11). As before, these equations are self-consistent. An example of this fact is the energy conservation equation

$$\frac{\partial}{\partial \tau} \sum_m |a_m|^2 = -2 \int \frac{dx\,dy}{\pi w_0^2} r \left\langle \frac{\partial \nu}{\partial \tau} \right\rangle_{\zeta_0 \nu_0} \tag{23}$$

which is derived from (17) and (19). The left-hand side of (23), the total energy gained by all the modes, is equal to the energy loss integrated over all of the electrons in the beam.

Equations (17–19) retain all of the generality of (1–3). They are valid for high and low fields, and high and low gain systems. They take into account the evolution of the transverse modes explicitly, and the evolution of the longitudinal modes implicitly, by keeping track of the $\hat{z}$ dependence of the charge density $r(\mathbf{r}, t)$ and of the mode amplitudes $a(z, t)$. For simplicity in the following development, we drop the explicit $\hat{z}$ dependence which has been thoroughly discussed by Colson [18], and concentrate on the transverse phenomena.

As discussed in [19], the generalization to the case of the planar undulator is no more than a change in the definition of the two parameters

$$a_m^{\text{lin}} = \frac{2\pi e N L K [JJ]}{\gamma^2 mc^2} c_m(t), \tag{24}$$

$$r^{\text{lin}} = \frac{4\pi^2 e^2 N L^2 K^2 [JJ]^2}{\gamma^3 mc^2} \varrho(\mathbf{r},t), \tag{25}$$

where

$$[JJ] \equiv J_0\left(\frac{K^2}{4+2K^2}\right) - J_1\left(\frac{K^2}{4+2K^2}\right). \tag{26}$$

Equations (17–19) can be integrated numerically to find the evolution of the optical wave in any Compton regime FEL. In a high-field experiment, (18) and (19) are nonlinear in a, and the wave evolution can only be obtained numerically. In this case, (17–19) provide a precise and efficient technique for solving the general

problem. In a low-field situation such as we find at Orsay, however, the problem becomes linear, and can be solved analytically. We proceed with the low field case in the next section.

2. The Low-Field Solution

The low-field case is defined by $|a_p| \ll 1$ for every mode. In other words, the electrons do not become overbunched. Experiments which operate in this domain include the low-field amplifier experiments, and storage ring FEL oscillators which saturate by mechanisms other than overbunching. The ignition of any FEL oscillator also occurs in this domain.

2.1. The Gain Matrix

Equations (17–19) can be solved by integrating (17) and (18) to lowest order in the fields a_m and inserting the result for ζ into (19). If the electrons are uniformly distributed initially in phase, we find

$$\frac{\partial a_m(\tau)}{\partial \tau} = \int_0^{\tau} d\tau' \int_0^{\tau'} d\tau'' M_{mn}(\tau, \tau'') a_n(\tau''), \tag{27}$$

where

$$M_{mn}(\tau, \tau'') = \frac{i}{2} \int \frac{dx\,dy}{\pi w_0^2} r(x, y)\, E_m(x, y, \tau)\, E_n(x, y, \tau'') \cdot e^{-i[(\psi_m(x, y, \tau) - \psi_n(x, y, \tau''))]} \langle e^{-i\nu_0(\tau - \tau'')} \rangle_{\nu_0}. \tag{28}$$

Equation (27) describes a linear evolution of the mode amplitudes, and upon integration, gives the relation

$$a_m(\tau = 1) = (I + G)_{mn} a_n(\tau = 0), \tag{29}$$

where I is the identity matrix, and G, which is generally not Hermitian, has elements

$$g_{mn} = \int_0^1 d\tau \int_0^{\tau} d\tau' \int_0^{\tau'} d\tau'' M_{mn}(\tau, \tau'') + \int_0^1 d\tau_1 \int_0^{\tau_1} d\tau_2 \int_0^{\tau_2} d\tau_3 M_{ml}(\tau_1, \tau_3) \cdot \int_0^{\tau_3} d\tau_4 \int_0^{\tau_4} d\tau_5 \int_0^{\tau_5} d\tau_6 M_{ln}(\tau_3, \tau_6) + \ldots. \tag{30}$$

The higher-order terms in g_{mn} are proportional to r^2 and higher powers of r, and are negligible in the low gain case.

Evidently this matrix is of great interest since multiple passes of the electron beam will result in multiple products of this matrix, greatly simplifying the calculation of the modes' growth. We shall discuss the consequences for an oscillation experiment in Sect. 2.2.

Let us note that this gain matrix is generally complex and defines the growth of the amplitude of the field. Sometimes people speak of the gain in a mode "m" as the energy gained by this mode in a pass through the undulator. This gain is simply $2\,\mathrm{Re}\{g_{mm}\} + |g_{mm}|^2$. Of course, one must keep in mind that energy is radiated into other modes, and that cross terms will mix a multiple mode input. If the input beam is truly monomode, the power radiated into the n^{th} mode is lower than that into the m^{th} mode by the ratio $|g_{mn}|^2/2\,\mathrm{Re}\{g_{mm}\}$ which is small for low gain ($r \ll 1$) systems. It is only in this case that it makes sense to speak of the gain of a mode. In high-gain systems, however, the off-diagonal terms can lead to substantial emission of energy into the higher-order transverse modes. If the input beam is multimode, of course, mode mixing occurs at all power levels.

Let us calculate g_{mn} in the simple case of experimental interest where the electron beam is cylindrical, and a good choice of modes is the cylindrical cavity eigenmodes (12) and (13). We restrict ourselves to the weakly diverging case $\pi w_0^2 \gg \lambda L$ where the gain takes on its most familiar form. The mode amplitudes and phases in (28) become independent of τ, and we can integrate the first term in (30) to find the gain. The average over the resonance parameter in (28) becomes, under the assumption of a Gaussian distribution of centroid ν_c and deviation σ_ν

$$\langle e^{-i\nu_0(\tau - \tau'')} \rangle_{\nu_0} = e^{-\frac{1}{2}\sigma_\nu^2(\tau - \tau'')^2} e^{-i\nu_c(\tau - \tau'')}. \tag{31}$$

Under the weak-divergence approximation, and assuming negligible pulse slippage effects (long electron bunch length $\sigma_l \gg N\lambda$), the only time-dependence in (28) is that of (31). For small spread $\sigma_\nu \ll 1$ the integral gives the well known gain spectrum

$$g_{mn} = \int \frac{dx\,dy}{\pi w_0^2} r(x, y)\, E_m(x, y)\, E_n(x, y)\, e^{-i\psi_m(x, y)}\, e^{i\psi_n(x, y)} \cdot \left\{ \frac{1 - \cos\nu_c - \frac{\nu_c}{2}\sin\nu_c}{\nu_c^3} + i \frac{-\frac{\nu_c}{2} - \frac{\nu_c}{2}\cos\nu_c + \sin\nu_c}{\nu_c^3} \right\}. \tag{32}$$

In the usual experimental case (unfortunately), $|g_{mn}| \ll 1$ and the energy gain G_m on the mode m becomes

$$G_m = 2\,\mathrm{Re}\{g_{mm}\} = \int \frac{dx\,dy}{\pi w_0^2} 2r E_m^2 \left(\frac{1 - \cos\nu_c - \frac{\nu_c}{2}\sin\nu_c}{\nu_c^3} \right). \tag{33}$$

This is exactly the gain one calculates by using the filling factor obtained by integrating the mode profile overlap with the gain profile. Specializing to the

TEM_{00} case with a Gaussian electron beam of width σ, we find

$$G_{00}=2r_0\left(\frac{1-\cos v_c-\frac{v_c}{2}\sin v_c}{v_c^3}\right)\frac{1}{1-\frac{w_0^2}{4\sigma^2}} \tag{34}$$

complete with the familiar filling factor.

The v_c dependence of G_m is the well known spectral dependence. The imaginary part of g_{mn} is not new. It describes the phase shift of the radiation field as described by Colson [18]. The inhomogeneous broadening term in (31) clearly distorts and reduces the magnitude of the gain spectrum if it is present in the integral of (30).

The effect of the divergence of the beam on the diagonal terms in G is, *to first order*, and for a filamentary electron beam, the addition of a time-varying phase which shifts the resonance curve in (32) by a constant depending on the mode

$$v_c \to v_c - \frac{\lambda L}{\pi w_0^2}(2p+l+1). \tag{35}$$

Equation (35) means that the gain curves of the modes are shifted with respect to each other. This effect has been calculated for the fundamental TEM_{00} mode in the energy loss approximation [14], and has recently been observed experimentally at Orsay [21]. It should be noted that for many practical situations where the cavity is optimized for gain on the TEM_{00} mode, this expression is valid for only the lowest-order mode. The higher modes become distorted in form as well as simply shifted in resonance parameter by (35).

2.2. *The Low-Field Oscillator*

We now discuss some consequence of the linearity of the low-field problem on the optimization of an optical cavity for an FEL oscillator experiment. In such an experiment the light pulses reflect n times on the cavity mirrors ($n \geqq 2$) between interactions with electrons in the undulator. The matrix governing the mode evolution from one amplification to the next is

$$(I+G)C, \tag{36}$$

where G in the gain matrix defined previously, and C is the cavity matrix describing the n reflections on the mirrors. In a set of cavity eigenmodes, C is diagonal

$$Cx^i=\mu_i x^i, \tag{37}$$

with $c_{jj}=\mu_j=\varrho_j \exp(\mathrm{i}\alpha_j)$, where $1-\varrho_j^2$ are the total losses on the n reflections, including transmission, absorption, scattering, and diffraction. If diffraction is negligible, the eigenvectors x^i become the Gaussian TEM_{pl} modes, and the phase shift per round trip α_i becomes, for $n=2$ reflections per amplification and identical radius of curvature mirrors, $\alpha_{pl}=4(2p+l+1)\tan^{-1}(L_c/2z_0)$, where L_c is the optical cavity length.

The matrix (36) is the fundamental matrix of the problem. Its diagonalization allows the calculation of the mode evolution up to the onset of saturation:

$$(I+G)C=PAP^{-1}, \tag{38}$$

$$[(I+G)C]^m=PA^mP^{-1}, \tag{39}$$

where the columns of P are composed of the eigenvectors of $(I+G)C$, and A is diagonal. The fastest mode growth will be obtained with the eigenmode having the highest eigenvalue modulus. Optimization of the FEL oscillator will then consist of maximizing the desired eigenvalue of $(I+G)C$.

If the gain is low (as it is, unfortunately, for our system on ACO), one can diagonalize the evolution matrix (36)

$$(I+G)Cz^i=\lambda_i z^i \tag{40}$$

using the cavity eigenmodes x^i as the basis for a perturbation expansion of the new modes z^i. To first order in the non-degenerate case, the result is

$$\lambda_j=\varrho_j e^{\mathrm{i}\alpha_j}(1+g_{jj}), \tag{41}$$

$$z^j=x^j+\sum_{m\neq j}\frac{\varrho_m e^{\mathrm{i}\alpha_m}}{\varrho_j e^{\mathrm{i}\alpha_j}-\varrho_m e^{\mathrm{i}\alpha_m}}g_{mj}x^m. \tag{42}$$

Under these conditions, the FEL design is optimized by maximizing the diagonal term g_{jj} corresponding to the desired mode. From (33) and (12) it is clear that the beam size w_0 must be reduced down to the order of the electron-beam size in order to optimize the coupling, but if the mode becomes too divergent, the time dependent terms in E_m and E_n of (28) begin to reduce the gain. The optimal situation lies between these two extremes, and has been calculated in detail (using the energy loss approximation) by Colson and Elleaume [14].

The optimization procedure must also be limited by the stability condition [17] on the cavity. For the Orsay experiment, the radius of curvature chosen to optimize the small-signal gain was $R=3\,\mathrm{m}$, which is acceptably close to the stability limit of 2.75 m. There are cavity designs in which C is degenerate for which the optimization procedure is not necessary. For these designs, α_j is a constant independent of the index. In these cavities, any combination of modes reproduces itself after n reflections. If $n=2$ as in the Stanford and the Orsay experiments, the concentric and the plane-parallel cavities are degenerate, and the confocal cavity is degenerate on the p modes (quasi-degenerate). These

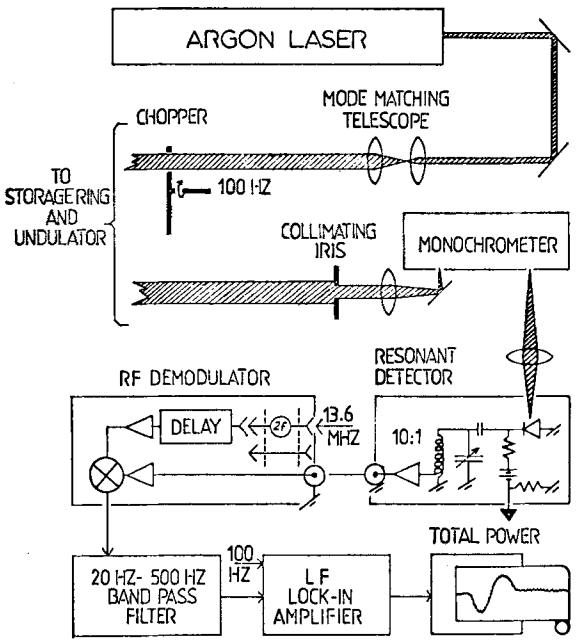

Fig. 1. Simplified schematic diagram of the gain-measurement apparatus [23] showing the argon-laser focussing system, the collimating iris, and the double demodulation detection system

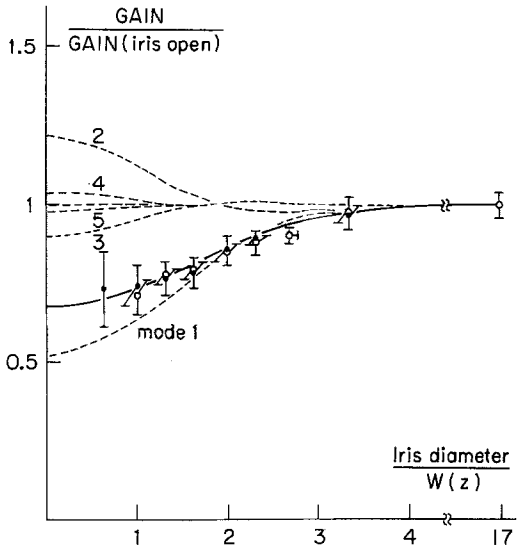

Fig. 2. The measured gain as a function of the iris diameter [16] normalized to the measured beam waist at the iris. The solid points were taken closing the iris and the open points while opening it. The error bars are the one sigma statistical errors. All points have the same horizontal error bar which is shown for the point at 2.7. The solid curve is calculated using the measured values for the electron and laser beam sizes. The effect of each higher-order mode is shown by the dashed curves

cavity designs, however, are useless since they stand critically on the stability boundary. The tolerance on the mirror radius of curvature is on the order of $|g_{00}|$ (obtained from the perturbation expansion) which is difficult to meet if the gain is low. For two-mirror devices where $n>2$, such as the Novosibirsk experiment where $n=8$, in general for mirrors of equal radius of curvature there exist $n/2+1$ cavity designs with a degenerate C matrix:

$$z_0=\frac{L_c}{2\tan\dfrac{m\pi}{n}} \tag{43}$$

and $n/2$ with a quasi-degenerate C matrix in which the odd l modes change sign on every amplification. Only two of the degenerate and one of the quasi-degenerate cavities correspond to the unstable cavities; the others are potentially useable in an experiment. The value of a degenerate C matrix is that the eigenvectors of the amplifier plus cavity matrix (36) are equal to those of the gain matrix alone, multiplied by a constant. This degeneracy allows the cavity to oscillate on the most favorable combination of modes which best fits the electron beam shape. In this manner, the gain can be increased by factors of two or three over the gain of an optimized TEM_{00} mode, particularly if the electron beam size is smaller than the TEM_{00} mode. The tolerance on the mirror radius for the degeneracy of C will still be tight, and the experimental utility of these cavities remains to be investigated.

3. Application to Gain-vs-Aperture Experiment

3.1. Description of the Experiment

The gain of the Orsay FEL has recently been measured with the optical klystron in place [22] in an amplifier experiment using an external argon ion laser to provide the coherent mode. A detailed description of the apparatus can be found in [23], and a schematic description is given in Fig. 1. The laser beam is analyzed at a distance d from the optical klystron after passing through an adjustable collimating iris (Fig. 1), which is centered on the laser mode emerging from the interaction region. The gain is measured as the ratio of the power detected in phase with both the electron repetition frequency and the chopper frequency (the amplified power) divided by the power in phase with the chopper alone (the incident laser power). Calibration is performed as in [23].

The again is recorded as a function of the iris aperture, and large variations are observed [16]. One set of data points is reproduced in Fig. 2, where the gain is normalized to its value for the iris completely open, and the iris diameter is normalized to the measured beam waist at the iris. The data is taken at maximum gain, which means $v_c\approx 0$ for the optical klystron, and

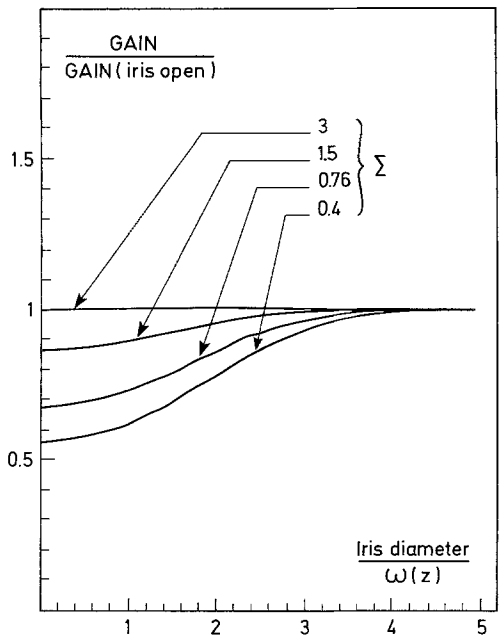

Fig. 3. Calculated curves for the gain as a function of iris diameter under the conditions of the Orsay experiment [16]. The electron beam dimension $\Sigma=\sigma\sqrt{\pi/\lambda L}$ is varied to show the effects of the beam size on the excitation of the higher order modes. The value $\Sigma=0.76$ corresponds to $\sigma=0.35$ mm which is very close to the value at which the experimental points were recorded

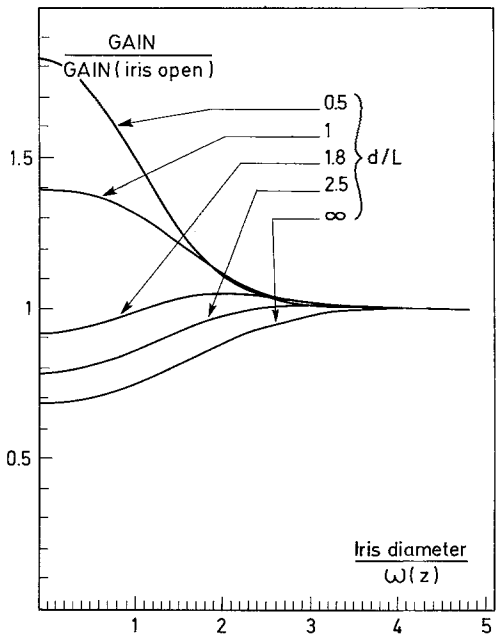

Fig. 4. Calculated gain as a function of iris diameter for several iris positions d, under the conditions of the Orsay experiment [16]. The ratio of the iris to optical klystron distance d divided by the optical klystron length L is varied through the range 0.5 to ∞. The experimental points of Fig. 2 were taken for $d/L=9$

the laser beam was carefully aligned to within about 0.05 mm of the axis of the electron beam. The change in the measured gain as the iris is closed means that the laser is not uniformly amplified in its transverse profile. In fact, this experiment provides a very sensitive technique for measuring the power emitted into the higher-order modes even in the small gain limit and for a monomode input beam. Clearly a calculation of the g_{mn} is necessary in order to explain these results. In the next section, we apply the theory we have developed to the case at hand, and in Sect. 3.3, precise comparison is made between the experimental and the theoretical results.

3.2. *Multimode Emission in a Single-Mode Amplifier Experiment*

In this subsection, we assume the incident wave is a single mode TEM_{00} beam with a weak field ($|a_0|<1$), and perfectly aligned onto the electron beam. As discussed previously, we take the cylindrical eigenmodes based on the form of the input beam. Using the notation of Sect. 1, the input laser field reads

$$E^I(\mathbf{r})=c_0E_0(\mathbf{r})e^{i\psi_0(\mathbf{r})}, \tag{44}$$

where the subscript 0 refers to the TEM_{00} mode of (12) and (13). From (29), the output field $E^s(\mathbf{r})$ becomes

$$E^s=E^I+c_0\sum_{j=0}^{\infty}g_{j0}E_j(\mathbf{r})e^{i\psi_j(\mathbf{r})}. \tag{45}$$

Assuming low gain, the output power passing through the iris aperture is

$$\frac{8\pi P}{c}=\int dS|E^s|^2\approx c_0^2\int dSE_0^2+2c_0^2\,\mathrm{Re}\cdot\left\{\sum_{j=0}^{\infty}g_{j0}\int dSE_0E_je^{i(\psi_0-\psi_j)}\right\}, \tag{46}$$

where $\int dS$ covers the iris aperture. The gain is therefore

$$G=\frac{2\,\mathrm{Re}\left\{\sum_{j=0}^{\infty}g_{j0}\int dSE_0E_je^{i(\psi_0-\psi_j)}\right\}}{\int dSE_0^2}. \tag{47}$$

For purely cylindrical $l=0$ modes, G can be written

$$G=2\,\mathrm{Re}\left\{g_{00}+\sum_{p=1}^{\infty}g_{p0}e^{i2p\tan^{-1}\frac{z}{z_0}}\frac{\int_0^X L_p(x)e^{-x}dx}{\int_0^X e^{-x}dx}\right\}, \tag{48}$$

where z_0 is the Rayleigh range of the laser mode, z is the distance between the iris and the laser beam waist, and $X=r_0^2/2w^2(z)$ where r_0 is the iris diameter. There

are two interesting limiting cases:

$$G = 2\,\mathrm{Re}\{g_{00}\} \quad X \to \infty \text{ (iris open)}, \tag{49}$$

$$G = 2\,\mathrm{Re}\left\{(g_{00}) + \sum_{p=1}^{\infty} g_{p0} e^{i2p\tan^{-1}\frac{z}{z_0}}\right\}$$

$$X \to 0 \text{ (iris closed)}. \tag{50}$$

It is obvious from (48–50) that the gain changes with iris diameter in a way which depends on the magnitudes of the off-diagonal terms in the gain matrix. The generalization is straightforward to the case of the multimode input beam, and to imperfect alignment of the laser and electron beams, although the calculation becomes more difficult. This calculation also applies to high-power input laser beams ($a_0 \gg 1$) provided one keeps in mind that the g_{p0} are functions of a_0.

3.3. *Application to the Orsay Experiment*

The experimental points shown on Fig. 2 were taken under the following approximate conditions

laser beam:
- measured beam waist $w_0 = 0.67$ mm
- wavelength = 5145 Å
- measured beam waist at iris $w(z) = 2.7$ mm
- distance from optical klystron to iris $d = 11.6$ m,

electron beam:
- Gaussian and cylindrical with $\sigma \simeq 0.32$ mm,

optical klystron:
- Nd = 80 [19, 22, 24]
- resonance parameter corresponding to maximum gain with iris open.

The solid curve of Fig. 2 has been calculated using (27, 28, and 50) for the planar configuration (24 and 25), taking into account the 10 lowest order $l = 0$ modes. The dashed curves of Fig. 2 show the contribution of each individual mode. These curves are the same whether an undulator or optical klystron is used. Very similar curves (not shown) were calculated for other resonance parameters indicating that as expected, the diffraction effects do not change much as a function of detuning parameter for modes with low divergence.

Figure 3 shows the calculated effect for several dimensionless electron beam transverse dimensions $\Sigma = \sqrt{\sigma\pi/\lambda L} = 0.4, 0.76, 1.5, 3$, where L is the length of the magnetic interaction region. $\Sigma = 0.76$ corresponds to the value $\sigma = 0.35$ mm, close to that used in Fig. 2. The flattening of the curves as Σ is increased to $\Sigma = 3$ is due to the vanishing of g_{0j}/g_{00} for $j \neq 0$ as σ increases.

Figure 4 shows the calculated effect for various iris distances d from the optical klystron center, normalized to the optical klystron length: $d/L = 0.5, 1, 1.8, 2.5$, and ∞. The experimental points of Fig. 2 were obtained for $d/L = 9$. The inversion of the effect is due primarily to the term $\exp[i2p\tan^{-1}(z/z_0)]$ with $p = 1$ in (50) which switches from $+1$ to -1 as z goes from zero to infinity (the mode $p = 1$ gives the predominant effect). At short distances the TEM_{10} mode interferes constructively on axis 1, and at long distances, it changes sign.

Acknowledgements. The authors would like to acknowledge stimulating discussions with W. B. Colson and J. M. J. Madey. The work was supported by the DRET, the Centre d'Etudes Nucleaires de Saclay DPC/SPP/SP, the Centre Nationale de la Recherche Scientifique, and was performed by Deacon Research under subcontract to HEPL, Stanford University, for the AFOSR.

References

1. D.A.G. Deacon, L.R. Elias, J.M.J. Madey, G.J. Ramian, H.A. Schwettman, T.I. Smith: Phys. Rev. Lett. **38**, 892 (1977)
2. IEEE J. QE-**17** (1981), Special Issue on Free-Electron Lasers (ed. by A. Szoke)
3. *Physics of Quantum Electronics*, Vols. 5 and 7–9 (Addison-Wesley, Reading, MA 1978–1982)
4. J.M.J. Madey et al.: Final Technical Report to ERDA: Contracts EY 76-S-03-0326 PA 48, and PA 49 (1977), available from the authors at HEPL, Stanford, CA 94305, USA
5. S. Benson, D.A.G. Deacon, J.N. Eckstein, J.M.J. Madey, K. Robinson, T.I. Smith, R. Taber: Phys. Rev. Lett. **48**, 235 (1982)
6. W.B. Colson, S.K. Ride: *Physics of Quantum Electronics* **7**, 377 (Addison-Wesley, Reading, MA 1980)
7. F.A. Hopf, T.G. Kuper, G.T. Moore, M.O. Scully: *Physics of Quantum Electronics* **7**, 31 (Addison-Wesley, Reading, MA 1980)
8. G. Dattoli, A. Marino, A. Renieri, F. Romanelli: IEEE J. QE-**17**, 1371 (1981)
9. C.-M. Tang, P. Sprangle: *Physics of Quantum Electronics* **9**, 627 (Addison-Wesley, Reading, MA 1982)
10. S.A. Mani, D.A. Korff, J. Blimmel: *Physics of Quantum Electronics* **9**, 557 (Addison-Wesley, Reading, MA 1982)
11. L.R. Elias, J.C. Gallardo: Phys. Rev. **24** A, 3276 (1981)
12. D. Prosnitz, R.A. Maas, S. Doss, R.J. Gelinas: *Physics of Quantum Electronics* **9**, 1047 (Addison-Wesley, Reading, MA 1982)
13. B.J. Coffey, M. Lax, C.J. Eliott: IEEE J. QE-**19**, 297 (1983)
14. W.B. Colson, P. Elleaume: Appl. Phys. B **29**, 101 (1982)
15. W.B. Colson, J.L. Richardson: Phys. Rev. Lett. **50**, 1050 (1983)
16. D.A.G. Deacon, J.-M. Ortega et al.: In preparation
17. A. Yariv: *Quantum Electronics* (Wiley, New York 1975) Chaps. 6 and 7
18. W.B. Colson: *Physics of Quantum Electronics* **8**, 457 (Addison-Wesley, Reading, MA 1982)
19. W.B. Colson: IEEE J. QE-**17**, 1417 (1981)
20. M. Kogelnik, T. Li: Proc. IEEE **54**, 1312 (1966)
21. D.A.G. Deacon et al.: In preparation
22. M. Billardon, D.A.G. Deacon, P. Elleaume, J.-M. Ortega et al.: In preparation
23. D.A.G. Deacon, J.M.J. Madey, K.E. Robinson, C. Bazin, M. Billardon, P. Elleaume, Y. Farge, J.-M. Ortega, Y. Petroff, M.F. Velghe: IEEE Trans. NS-**28**, 3142 (1981)
24. P. Elleaume: J. Phys. (Paris) **44**, C1–333 (1983)